DOI: 10.1002/ange.201408831

Donor–Acceptor Systems

Organic Donor–Acceptor Assemblies form Coaxial p–n Heterojunctions with High Photoconductivity**

*Seelam Prasanthkumar, Samrat Ghosh, Vijayakumar C. Nair, Akinori Saeki, Shu Seki, and Ayyappanpillai Ajayaghosh**

Abstract: *The formation of coaxial p–n heterojunctions by mesoscale alignment of self-sorted donor and acceptor molecules, important to achieve high photocurrent generation in organic semiconductor-based assemblies, remains a challenging topic. Herein, we show that mixing a p-type π gelator (TTV) with an n-type semiconductor (PBI) results in the formation of self-sorted fibers which are coaxially aligned to form interfacial p–n heterojunctions. UV/Vis absorption spectroscopy, powder X-ray diffraction studies, atomic force microscopy, and Kelvin-probe force microscopy revealed an initial self-sorting at the molecular level and a subsequent mesoscale self-assembly of the resulted supramolecular fibers leading to coaxially aligned p–n heterojunctions. A flash photolysis time-resolved microwave conductivity (FP-TRMC) study revealed a 12-fold enhancement in the anisotropic photoconductivity of TTV/PBI coaxial fibers when compared to the individual assemblies of the donor/acceptor molecules.*

Self-assembled, one-dimensional (1D) donor–acceptor nanostructures are of interest as a result of their unidirectional charge-transport properties,[1] thereby serving as an integral part in organic bulk-heterojunction (BHJ) solar cells.[2] To improve the charge-carrier generation and transport properties in solution-processed BHJs, nanostructures should have optimal phase separation, preferably with lateral organization of donor–acceptor moieties.[3] However, control of the assembly of organic donor–acceptor semiconductors to form 1D supramolecular fibers which have coaxially aligned heterojunctions is a difficult task. Self-sorted assemblies of electron-donor (D) and electron-acceptor (A) molecules provide ample scope for facilitating photocurrent generation whereas formation of charge-transfer (CT) complexes inhibit photocurrent through recombination.[4] In this context, several approaches have been reported to achieve p–n heterojunctions in 1D nanostructures.[5,6]

Self-assembly is known to be a promising strategy to organize functional molecules into supramolecular architectures of different sizes, shapes, and properties.[7,8] However, self-assembly of donor–acceptor organic semiconductors generally results in the formation of mixed stacks (Scheme 1, path a).[9] Under restricted conditions, they can form self-sorted assemblies leading to entangled fibers with localized heterojunctions (path b)[10] or aligned fibers with interfacial heterojunctions (path c). For better charge separation, path c is preferred. With this objective, we propose the concept of a self-sorting approach at the molecular level followed by self-assembly at the mesoscale, leading to the formation of interfacial p–n heterojunctions. As a proof of principle to this hypothesis, herein we demonstrate the creation of self-sorted supramolecular 1D nanostructures of a p-type gelator and an n-type semiconductor with coaxially aligned p–n heterojunctions with high photoconductivity.

Recently, we reported that trithienylenevinylene molecules with amide end functional groups form supramolecular gels in nonpolar solvents.[11] These derivatives exhibited excellent electron-donating properties and high charge-carrier mobility in the self-assembled state. This observation motivated us to investigate further the charge-carrier generation and transport properties of the materials in the presence of suitable n-type semiconductors. In the present work, we have selected a trithienylenevinylene derivative (TTV) as the donor (p-type) and a structurally dissimilar perylene bisimide (PBI)[12–14] as the acceptor (n-type; Figure 1). PBI was selected as the n-type material because of its suitable HOMO–LUMO energy gap with respect to that of TTV.

The UV/Vis absorption spectra of TTV, PBI, and TTV/PBI (1:1 molar ratio) were recorded in chloroform and *n*-decane at a concentration of 1×10^{-4} M (see Figure 1c for the spectra in *n*-decane). TTV exhibits an absorption band maximum at around $\lambda = 501$ nm in chloroform (Figure S1d in the Supporting Information). This absorption band underwent a blue shift to $\lambda = 464$ nm ($\Delta\lambda = 37$ nm) in *n*-decane, indicating that the molecule has undergone strong H-type 1D aggregation.[11,15] The absorption spectrum of PBI in chloroform showed sharp absorption bands at $\lambda = 458$, 491, and 526 nm. In *n*-decane, these characteristic bands are also

[*] Dr. S. Prasanthkumar, S. Ghosh, Dr. V. C. Nair, Prof. Dr. A. Ajayaghosh
Photosciences and Photonics Group
Chemical Sciences and Technology Division
CSIR-National Institute for Interdisciplinary Science and Technology (CSIR-NIIST), Trivandrum-695019 (India)
S. Ghosh, Dr. V. C. Nair, Prof. Dr. A. Ajayaghosh
Academy of Scientific and Innovative Research (AcSIR)
CSIR-National Institute for Interdisciplinary Science and Technology (CSIR-NIIST), Trivandrum-695019 (India)
E-mail: ajayaghosh@niist.res.in
Dr. A. Saeki, Prof. Dr. S. Seki
Department of Applied Chemistry
Graduate School of Engineering, Osaka University
2-1 Yamadaoka, Suita, Osaka 565-0871 (Japan)

[**] We thank the Council of Scientific and Industrial Research (CSIR), Government of India for financial support under NWP-54 and Department of Science and Technology (DST), Government of India for an exchange project under the DST-JSPS programme.

Supporting information for this article is available on the WWW under http://dx.doi.org/10.1002/anie.201408831.

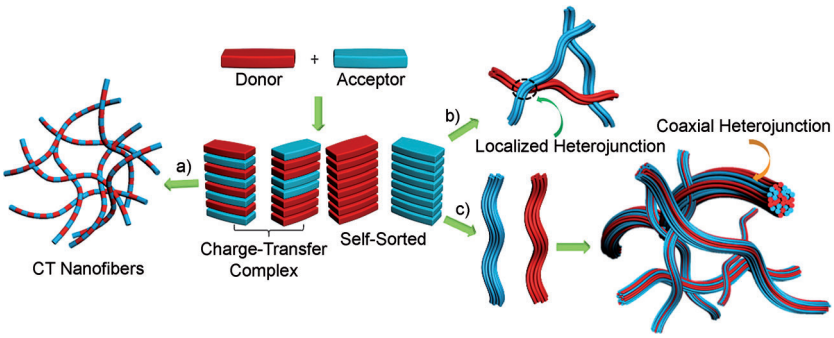

Scheme 1. A conceptual representation showing the possible interactions between a p-type donor and an n-type acceptor leading to different possible hierarchical structures.

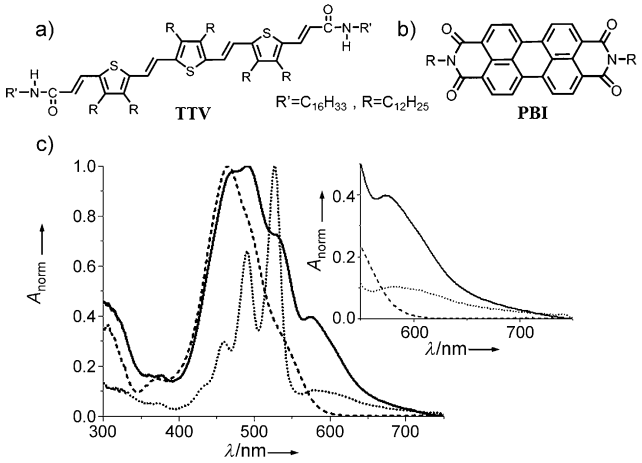

Figure 1. Chemical structure of a) TTV (p-type material) and b) PBI (n-type material). c) UV/Vis absorption spectra of TTV (dashed line), PBI (dotted line), and a mixture of TTV/PBI in a 1:1 molar ratio (solid line) in *n*-decane ($c = 1 \times 10^{-4}$ M). Inset: expanded portion of the absorption spectrum from $\lambda = 550$ to 750 nm.

detected in addition to a shoulder band at around $\lambda = 580$ nm, typical of a J-type aggregation (Figure 1c).[16] Mixing TTV and PBI in a 1:1 molar ratio in *n*-decane or in chloroform gave rise to UV/Vis absorption spectra which retained the individual absorption spectral features of the two components (see Figure 1c and Figure S1d for spectra in *n*-decane and chloroform, respectively). Considering the electron-donating ability of TTV and electron-accepting ability of PBI, the molecules would be expected to form a CT complex.

In the case of the mixed solution of TTV/PBI (1:1 molar ratio), a strong CT interaction is ruled out because of the absence of any new absorption band or band shift in the UV/Vis absorption spectrum. The contrasting structural features of the molecules may discourage a direct CT interaction between the two molecules. In the case of TTV, because of the directional hydrogen-bonding interaction, the propensity for 1D self-assembly is very strong. On the other hand, large π-surface-induced stacking is the major force in the self-assembly of PBI molecules. In this system, self-sorting may be preferred as 1D hydrogen bonding leads to a H-type packing in TTV and π–π stacking leads to a J-type arrangement in PBI. Variable-temperature UV/Vis absorption spectral studies in *n*-decane revealed the characteristics of their individual transitions upon heating from 20–70 °C (Figure S1c). However, as the possibility of CT formation cannot be completely ruled out by UV/Vis spectral data, we performed morphological and powder X-ray diffraction (XRD) studies to check for any evidence for CT formation.

Atomic force microscopy (AFM) and transmission electron microscopy (TEM) images of TTV drop-cast from an *n*-decane solution ($c = 5 \times 10^{-5}$ M) onto silicon wafer or carbon-coated copper grids revealed the formation of entangled fibers (Figures 2a and d, respectively). The average diameters of these nanofibers are in the range of 50–200 nm with a height of 40–80 nm. On the other hand, PBI films showed the formation of elongated sheets of several micrometers in length (Figures 2b and e). It is interesting to note that the morphology of the mixed assembly was different from those of the individual

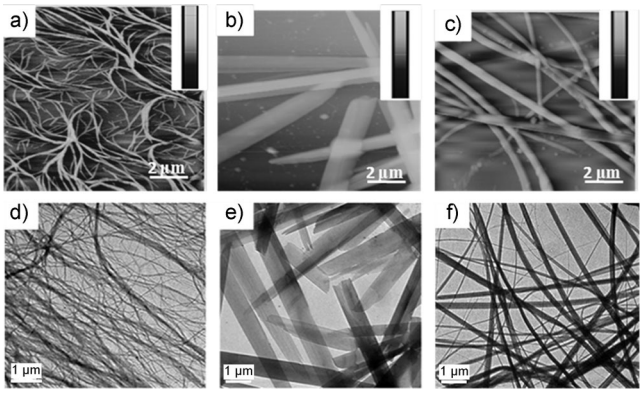

Figure 2. AFM images of a) TTV, b) PBI, and c) TTV/PBI (1:1 molar ratio) drop cast from *n*-decane solutions ($c = 5 \times 10^{-5}$ M) on a silicon wafer at room temperature. Z-scale corresponds to a) 60 nm, b) 200 nm, and c) 300 nm, respectively. TEM images of d) TTV, e) PBI, and f) TTV/PBI (1:1 molar ratio) drop-cast from *n*-decane solutions ($c = 5 \times 10^{-5}$ M) onto carbon-coated copper grids at room temperature. Scale bar in (a–c) = 2 μm; scale bar in (d–f) = 1 μm.

TTV and PBI assemblies. The TTV/PBI mixture exhibited rod-like structures with lengths of micrometers having diameter of 300–500 nm (Figures 2c and f). These long rods might be formed by the bundling of short fibers of 40–70 nm as evidenced from the TEM image. In the case of self-sorting, the presence of a mixture of individual stacks of TTV and PBI would be expected in the AFM and TEM images. The fact that the morphology observed in the microscopic images was completely different to that of the individual stacks suggests the formation of a coassembly as shown in Scheme 1, path a. However, the absence of a CT band in the UV/Vis absorption spectrum ruled out this possibility. Therefore, it could be inferred that the initially formed self-sorted stacks of the 1:1 mixture of TTV and PBI could subsequently self-assemble to form hierarchical structures which resembles neither the

donor assembly nor the acceptor assembly. The weak opposite charges of the self-sorted donor and acceptor fibers facilitate interfacial interaction at the nanoscale to form coaxially aligned mesoscale fiber bundles (Scheme 1, path c).

Powder X-ray diffraction (XRD) analysis of the TTV xerogel film (Figure 3) showed an amorphous pattern with

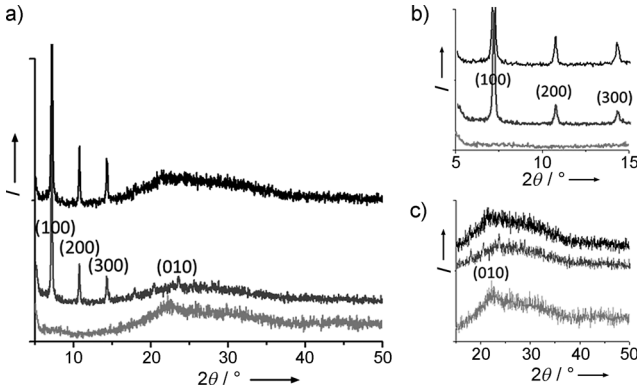

Figure 3. a) Powder XRD pattern of TTV (light gray), PBI (dark gray), and TTV/PBI (black) in the self-assembled film state. Expanded portion of the XRD pattern between b) $2\theta = 5$–$15°$ and c) $2\theta = 15$–$50°$.

a broad peak around $2\theta = 23.1°$. This peak corresponds to a d spacing of 3.8 Å which indicates the π–π stacking distance between the TTV molecules. In the case of PBI, the characteristic and distinct sharp diffraction peaks with d spacings of 12.4 Å (100), 8.3 Å (200), 6.2 Å (300), and 3.1 Å (010) were obtained. The mixture of TTV/PBI (1:1 molar ratio) showed a diffraction pattern which is a combination of those of the individual TTV and PBI patterns. Diffraction peaks at 12.3 Å (100), 8.2 Å (200), 6.2 Å (300), and 3.3 Å (010) in the mixture pattern match with those of the PBI pattern. The absence of any new peak or peak shift in the XRD pattern of the mixed assemblies reveals that TTV and PBI molecules preferentially form individual stacks during the mixing. These data reconfirm the hypothesis that a molecular-level self-sorting occurs between the donor and the acceptor at the initial stage and that they subsequently interact to form mesoscopic coaxially aligned donor–acceptor fiber bundles with interfacial p–n heterojunctions.[6d]

Having confirmed the mode of interaction between TTV and PBI, we performed Kelvin-probe force microscopy (KPFM) which is a useful tool to measure the electric surface potential (SP) of donor–acceptor assemblies with nanoscale resolution.[17] TTV exhibits a surface potential of 15 ± 5 mV in open air and under ambient-light conditions (Figure S2). The surface potential of PBI was in the range of -40 ± 5 mV (Figure S3). Figure 4a and b show the AFM topography and the corresponding KPFM image of the TTV/PBI mixture (1:1 molar ratio) which showed elongated fibers with diameter of 300–500 nm and height of 100–200 nm. The corresponding surface-potential value (SP) obtained from section analysis was -100 ± 10 mV. These data suggest that the mixed assembly exhibits a large shift in the surface-potential values when compared to the individual assemblies of TTV

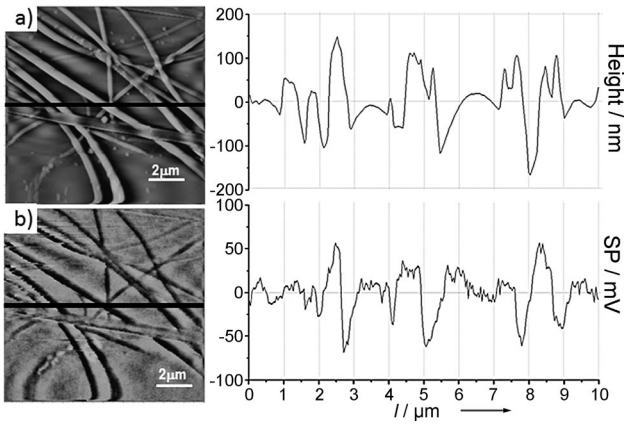

Figure 4. a) AFM and b) KPFM images of a TTV/PBI mixture (1:1 molar ratio) drop-cast from an *n*-decane solution ($c = 5 \times 10^{-5}$ M) onto a silicon wafer at room temperature. Corresponding section analysis shown on the right. SP = surface potential.

and PBI, further indicating that there is effective phase segregation at the nanoscale between the self-sorted donor and acceptor species.

To study how the coaxially aligned p–n heterojunctions affect the photoconductivity properties in the case of the TTV/PBI mixed assembly, we have carried out flash photolysis time-resolved microwave conductivity (FP-TRMC) experiments.[18] The intrinsic photoconductivity property of the materials could be quantified from the $\phi\Sigma\mu$ values, obtained from FP-TRMC, where ϕ is the charge-carrier-generation quantum yield upon photoexcitation and $\Sigma\mu$ is the sum of charge-carrier mobilities, that is, the sum of electron and hole mobility. The maximum value ($\phi\Sigma\mu_{max}$) reflects the intrinsic photoconductivity of the material with minimum trapping effects. The FP-TRMC data in many cases usually reflects the intrinsic short-range charge-carrier mobility. However, in some cases, this intrinsic photoconductivity can be correlated to bulk properties, such as device performances.[19] First, we investigated the intrinsic charge-carrier mobility of the TTV xerogel film by a combination of FP-TRMC and transient absorption spectroscopy (TAS; Figure S4). It was found that the minimum charge-carrier mobility ($\Sigma\mu_{min}$) of TTV in the self-assembled state was 0.14 $cm^2 V^{-1} s^{-1}$. This value indicates that self-assembled TTV has excellent charge-carrier mobility which is comparable to that of P3HT (poly(3-hexylthiophene)).[18b] This efficient carrier transport suggests the formation of coaxial heterojunctions as depicted in Figure 1c.

The FP-TRMC transients of TTV/PBI (1:1 molar ratio) were measured and compared with that of TTV and PBI assemblies (Figure 5a). TTV/PBI (1:1 molar ratio) shows an almost 12-fold enhancement in $\phi\Sigma\mu$ values with respect to TTV. This study confirms that the formation of coaxial p–n heterojunctions significantly enhances the photoconductivity in donor–acceptor assemblies. This could be attributed to the enhancement in ϕ values rather than $\Sigma\mu$ values, because the coaxial organization of donors and acceptors facilitate charge separation, whereas the ability of the assemblies to transport charge ($\Sigma\mu$) is expected to remain

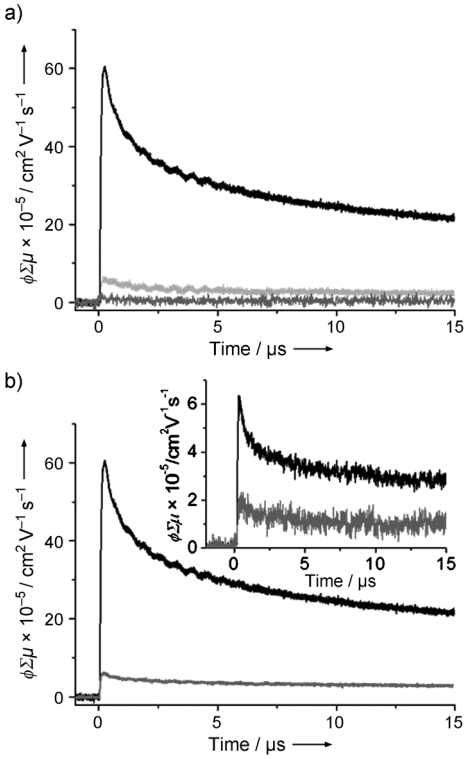

Figure 5. FP-TRMC photoconductivity transient spectra of a) TTV (light gray), PBI (dark gray), and TTV/PBI (1:1 molar ratio; black) films. b) FP-TRMC photoconductivity spectra of a TTV/PBI film (1:1 molar ratio) prepared from *n*-decane (inset: spectra prepared from chloroform) showing parallel ($\phi\Sigma\mu_{\parallel}$; black) and perpendicular ($\phi\Sigma\mu_{\perp}$; dark gray) alignment of the film with that of the microwave electric-field vector upon $\lambda = 355$ nm laser excitation at 9.1×10^{15} photon cm^{-2}.

same. Furthermore, anisotropic photoconductivity measurements have been performed for TTV/PBI films processed from chloroform as well as *n*-decane solutions. Figure 5b shows $\phi\Sigma\mu$ values measured for the parallel ($\phi\Sigma\mu_{\parallel}$) and perpendicular ($\phi\Sigma\mu_{\perp}$) alignment of the film with respect to the direction of the microwave electric-field vector. The film processed from chloroform showed a low anisotropic photoconductivity (ca. $\phi\Sigma\mu_{\parallel}$:$\phi\Sigma\mu_{\perp} = 3$:1, see Figure 5b, inset), whereas higher anisotropic photoconductivity ($\phi\Sigma\mu_{\parallel}$:$\phi\Sigma\mu_{\perp} =$ 12:1) was obtained for the self-assembled film (processed from *n*-decane, Figure 5b). The higher value of $\phi\Sigma\mu_{\parallel}$ in the self-assembled state reveals that the majority of the donor and acceptor molecules are unidirectionally aligned, underpinning our interpretation of the mesoscopic co-assembly of the molecularly self-sorted structures.

In summary, a combined self-sorting and self-assembly approach is employed for the construction of coaxially aligned supramolecular fibers of a p-type gelator with an n-type semiconductor, resulting in the formation of 1D interfacial p–n heterojunctions. Such coaxial interfacial heterojunctions are ideal to generate high photoconductivity. Formation of coaxial heterojunctions is demonstrated by UV/Vis absorption spectra, microscopic, XRD, and FP-TRMC studies. Even though we could achieve high photoconductivity, for efficient charge collection in a conventional device structure, vertical placement of such coaxial fibers between electrodes is essential. However, this vertical placement is difficult to achieve in self-assembled donor–acceptor systems. Until and unless we solve this issue, the target of achieving high device performances using organic donor–acceptor assemblies remains challenging.

Received: September 5, 2014
Revised: October 24, 2014
Published online: November 27, 2014

Keywords: donor–acceptor systems · photoconductivity · p–n heterojunctions · self-assembly · self-sorting

[1] a) T. Aida, E. W. Meijer, S. I. Stupp, *Science* **2012**, *335*, 813 – 817; b) F. S. Kim, G. Q. Ren, S. A. Jenekhe, *Chem. Mater.* **2011**, *23*, 682 – 732; c) L. C. Palmer, S. I. Stupp, *Acc. Chem. Res.* **2008**, *41*, 1674 – 1684; d) J. D. Hartgerink, E. Beniash, S. I. Stupp, *Science* **2001**, *294*, 1684 – 1688; e) F. J. M. Hoeben, P. Jonkheijm, E. W. Meijer, A. P. H. J. Schenning, *Chem. Rev.* **2005**, *105*, 1491 – 1546; f) A. P. Alivisatos, *Science* **1996**, *271*, 933 – 937.

[2] a) A. Mishra, P. Bäuerle, *Angew. Chem. Int. Ed.* **2012**, *51*, 2020 – 2067; *Angew. Chem.* **2012**, *124*, 2060 – 2109; b) G. Li, R. Zhu, Y. Yang, *Nat. Photonics* **2012**, *6*, 153 – 161; c) N. S. Dang, L. Hirsch, G. Wantz, J. D. Wuest, *Chem. Rev.* **2013**, *113*, 3734 – 3765; d) Y. Lin, Y. Li, X. Zhan, *Chem. Soc. Rev.* **2012**, *41*, 4245 – 4272.

[3] a) J. J. M. Halls, C. A. Walsh, N. C. Greenham, E. A. Marseglia, R. H. Friend, S. C. Moratti, A. B. Holmes, *Nature* **1995**, *376*, 498 – 500; b) G. Yu, J. Gao, J. C. Hummelen, F. Wudl, A. J. Heeger, *Science* **1995**, *270*, 1789 – 1791; c) P. Peumans, S. Uchida, S. R. Forrest, *Nature* **2003**, *425*, 158 – 162; d) J. Y. Kim, K. Lee, N. E. Coates, D. Moses, T. Q. Nguyen, M. Dante, A. J. Heeger, *Science* **2007**, *317*, 222 – 225; e) L. Dong, W. Li, W.-S. Li, *Nanoscale* **2011**, *3*, 3447 – 3461.

[4] a) J. M. Lehn, *Supramolecular Chemistry: Concepts and Perspectives*, Wiley, New York, **1995**, pp. 139 – 198; b) M. M. Safont-Sempere, G. Fernández, F. Würthner, *Chem. Rev.* **2011**, *111*, 5784 – 5814; c) A. Das, S. Ghosh, *Angew. Chem. Int. Ed.* **2014**, *53*, 2038 – 2054; *Angew. Chem.* **2014**, *126*, 2068 – 2084; d) S. S. Babu, S. Prasanthkumar, A. Ajayaghosh, *Angew. Chem. Int. Ed.* **2012**, *51*, 1766 – 1776; *Angew. Chem.* **2012**, *124*, 1800 – 1810.

[5] a) W. Zhang, W. Jin, T. Fukushima, A. Saeki, S. Seki, T. Aida, *Science* **2011**, *334*, 340 – 343; b) R. Bhosale, J. Misek, N. Sakai, S. Matile, *Chem. Soc. Rev.* **2010**, *39*, 138 – 149; c) J. van Herrikhuyzen, A. Syamakumari, A. P. H. J. Schenning, E. W. Meijer, *J. Am. Chem. Soc.* **2004**, *126*, 10021 – 10027; d) D. M. Bassani, L. Jonusauskaite, A. Lavie-Cambot, N. D. McClenaghan, J. L. Pozzo, D. Ray, G. Vives, *Coord. Chem. Rev.* **2010**, *254*, 2429 – 2445.

[6] a) F. Würthner, Z. Chen, F. J. M. Hoeben, P. Osswald, C. C. You, P. Jonkheijm, J. van Herrikhuyzen, A. P. H. J. Schenning, P. P. A. M. van der Schoot, E. W. Meijer, E. H. A. Beckers, S. C. J. Meskers, R. A. J. Janssen, *J. Am. Chem. Soc.* **2004**, *126*, 10611 – 10618; b) H. Huang, C. E. Chou, Y. Che, L. Li, C. Wang, X. Yang, Z. Peng, L. Zang, *J. Am. Chem. Soc.* **2013**, *135*, 16490 – 16496; c) L. Bu, E. Pentzer, F. A. Bokel, T. Emrick, R. C. Hayward, *ACS Nano* **2012**, *6*, 10924 – 10929; d) M. Brinkmann, E. Gonthier, S. Bogen, K. Tremel, S. Ludwigs, M. Hufnagel, M. Sommer, *ACS Nano* **2012**, *6*, 10319 – 10326.

[7] a) A. Ajayaghosh, V. K. Praveen, *Acc. Chem. Res.* **2007**, *40*, 644 – 656; b) A. Ajayaghosh, V. K. Praveen, C. Vijayakumar, *Chem. Soc. Rev.* **2008**, *37*, 109 – 122; c) V. K. Praveen, C. Ranjith, E. Bandini, A. Ajayaghosh, N. Armaroli, *Chem. Soc. Rev.* **2014**, *43*, 4222 – 4242; d) K. K. Kartha, R. D. Mukhopadhyay, A. Ajayaghosh, *Chimia* **2013**, *67*, 51 – 63; e) S. S. Babu, V. K. Praveen, A. Ajayaghosh, *Chem. Rev.* **2014**, *114*, 1973 – 2129; f) M. R. Molla,

A. Das, S. Ghosh, *Chem. Eur. J.* **2010**, *16*, 10084 – 10093; g) E. Busseron, Y. Ruff, E. Moulin, N. Giuseppone, *Nanoscale* **2013**, *5*, 7098 – 7140.

[8] a) A. Ajayaghosh, S. J. George, V. K. Praveen, *Angew. Chem. Int. Ed.* **2003**, *42*, 332 – 335; *Angew. Chem.* **2003**, *115*, 346 – 349; b) V. K. Praveen, S. J. George, R. Varghese, C. Vijayakumar, A. Ajayaghosh, *J. Am. Chem. Soc.* **2006**, *128*, 7542 – 7550; c) A. Ajayaghosh, V. K. Praveen, S. Srinivasan, R. Varghese, *Adv. Mater.* **2007**, *19*, 411 – 415; d) C. Vijayakumar, V. K. Praveen, A. Ajayaghosh, *Adv. Mater.* **2009**, *21*, 2059 – 2063; e) S. S. Babu, K. K. Kartha, A. Ajayaghosh, *J. Phys. Chem. Lett.* **2010**, *1*, 3413 – 3424; f) F. García, J. Buendìa, S. Ghosh, A. Ajayaghosh, L. Sánchez, *Chem. Commun.* **2013**, *49*, 9278 – 9280; g) S. Santhosh Babu, J. Aimi, H. Ozawa, N. Shirahata, A. Saeki, S. Seki, A. Ajayaghosh, H. Möhwald, T. Nakanishi, *Angew. Chem. Int. Ed.* **2012**, *51*, 3391 – 3395; *Angew. Chem.* **2012**, *124*, 3447 – 3451.

[9] a) K. P. Goetz, D. Vermeulen, M. E. Payne, C. Kloc, L. E. McNeil, O. D. Jurchescu, *J. Mater. Chem. C* **2014**, *2*, 3065 – 3076; b) K. Jalani, M. Kumar, S. J. George, *Chem. Commun.* **2013**, *49*, 5174 – 5176; c) P. Jonkheijm, N. Stutzmann, Z. Chen, D. M. de Leeuw, E. W. Meijer, A. P. H. J. Schenning, F. Würthner, *J. Am. Chem. Soc.* **2006**, *128*, 9535 – 9540; d) L. F. Dössel, V. Kamm, I. A. Howard, F. Laquai, W. Pisula, X. Feng, C. Li, M. Takase, T. Kudernac, S. De Feyter, K. Müllen, *J. Am. Chem. Soc.* **2012**, *134*, 5876 – 5886.

[10] a) K. Sugiyasu, S. I. Kawano, N. Fujita, S. Shinkai, *Chem. Mater.* **2008**, *20*, 2863 – 2865; b) A. Wicklein, S. Ghosh, M. Sommer, F. Würthner, M. Thelakkat, *ACS Nano* **2009**, *3*, 1107 – 1114.

[11] a) S. Prasanthkumar, A. Saeki, S. Seki, A. Ajayaghosh, *J. Am. Chem. Soc.* **2010**, *132*, 8866 – 8867; b) S. Prasanthkumar, A. Gopal, A. Ajayaghosh, *J. Am. Chem. Soc.* **2010**, *132*, 13206 – 13207.

[12] a) D. Görl, X. Zhang, F. Würthner, *Angew. Chem. Int. Ed.* **2012**, *51*, 6328 – 6348; *Angew. Chem.* **2012**, *124*, 6434 – 6455; b) F. Würthner, *Chem. Commun.* **2004**, 1564 – 1579; c) T. E. Kaiser, H. Wang, V. Stepanenko, F. Würthner, *Angew. Chem. Int. Ed.* **2007**, *46*, 5541 – 5544; *Angew. Chem.* **2007**, *119*, 5637 – 5640.

[13] a) Y. Wen, Y. Liu, *Adv. Mater.* **2010**, *22*, 1331 – 1345; b) X. Zhan, Z. Tan, B. Domercq, Z. An, X. Zhang, S. Barlow, Y. Li, D. Zhu, B. Kippelen, S. R. Marder, *J. Am. Chem. Soc.* **2007**, *129*, 7246 – 7247.

[14] K. Balakrishnan, A. Datar, T. Naddo, J. Huang, R. Oitker, M. Yen, J. Zhao, L. Zang, *J. Am. Chem. Soc.* **2006**, *128*, 7390 – 7398.

[15] a) F. C. Spano, *Acc. Chem. Res.* **2009**, *42*, 429 – 439; b) A. Ajayaghosh, C. Vijayakumar, R. Varghese, S. J. George, *Angew. Chem. Int. Ed.* **2006**, *45*, 456 – 460; *Angew. Chem.* **2006**, *118*, 470 – 474; c) U. Rösch, S. Yao, R. Wortmann, F. Würthner, *Angew. Chem. Int. Ed.* **2006**, *45*, 7026 – 7030; *Angew. Chem.* **2006**, *118*, 7184 – 7188.

[16] F. Würthner, T. E. Kaiser, C. R. Saha-Möller, *Angew. Chem. Int. Ed.* **2011**, *50*, 3376 – 3410; *Angew. Chem.* **2011**, *123*, 3436 – 3473.

[17] a) A. Liscio, V. Palermo, P. Samorì, *Adv. Funct. Mater.* **2008**, *18*, 907 – 914; b) A. Liscio, V. Palermo, P. Samorì, *Acc. Chem. Res.* **2010**, *43*, 541 – 550; c) A. Liscio, G. De Luca, F. Nolde, V. Palermo, K. Müllen, P. Samorì, *J. Am. Chem. Soc.* **2008**, *130*, 780 – 781; d) V. Palermo, M. B. J. Otten, A. Liscio, E. Schwartz, P. A. J. de Witte, M. A. Castriciano, M. M. Wienk, F. Nolde, G. De Luca, J. J. L. M. Cornelissen, R. A. J. Janssen, K. Müllen, A. E. Rowan, R. J. M. Nolte, P. Samorì, *J. Am. Chem. Soc.* **2008**, *130*, 14605 – 14614; e) F. Fuchs, M. Linares, C. de Vet, P. Leclère, R. Demadrille, B. Grévin, *Adv. Mater.* **2014**, *26*, 6416 – 6422.

[18] a) A. Saeki, S. Seki, T. Takenobu, Y. Iwasa, S. Tagawa, *Adv. Mater.* **2008**, *20*, 920 – 923; b) A. Saeki, S.-i. Ohsaki, S. Seki, S. Tagawa, *J. Phys. Chem. C* **2008**, *112*, 16643 – 16650; c) Y. He, Y. Yamamoto, W. Jin, T. Fukushima, A. Saeki, S. Seki, N. Ishii, T. Aida, *Adv. Mater.* **2010**, *22*, 829 – 832; d) A. Saeki, Y. Koizumi, T. Aida, S. Seki, *Acc. Chem. Res.* **2012**, *45*, 1193 – 1202.

[19] a) A. Saeki, M. Tsuji, S. Seki, *Adv. Energy Mater.* **2011**, *1*, 661 – 669; b) A. Saeki, S. Yoshikawa, M. Tsuji, Y. Koizumi, M. Ide, C. Vijayakumar, S. Seki, *J. Am. Chem. Soc.* **2012**, *134*, 19035 – 19042; c) B. Balan, C. Vijayakumar, A. Saeki, Y. Koizumi, M. Tsujia, S. Seki, *Polym. Chem.* **2013**, *4*, 2293 – 2303; d) W. A. Braunecker, S. D. Oosterhout, Z. R. Owczarczyk, R. E. Larsen, B. W. Larson, D. S. Ginley, O. V. Boltalina, S. H. Strauss, N. Kopidakis, D. C. Olson, *Macromolecules* **2013**, *46*, 3367 – 3375.

